journal

J. Am. Ceram. Soc., 76 [11] 2727–33 (1993)

Preparation of Composite Particles by Pulsed Nd-YAG Laser Decomposition of $[(CH_3)_2N]_4Ti$ to TiN-Coat TiO_2, Al_2O_3, or Si_3N_4 Powders

Chaitanya K. Narula,*,§ M. Matti Maricq,* Brian G. Demczyk,† Irving T. Salmeen,* and Willes H. Weber‡

Chemistry Department and Physics Department, Ford Motor Company, Dearborn, Michigan 48121-2053
Electron Microbeam Analysis Laboratory, The University of Michigan, Ann Arbor, Michigan 48109

Irradiation of $Ti[N(CH_3)_2]_4$ by the 1.064-μm line of a pulsed Nd:YAG laser in the presence of TiO_2, Al_2O_3, or Si_3N_4 particles has been found to form amorphous deposits on the oxide particles. The resulting materials can be processed into TiN/TiO_2, TiN/Al_2O_3, or TiN/Si_3N_4 composites with the TiN component on the surface of the particles. The powders have been characterized by Raman spectroscopy and X-ray powder diffraction studies. The surface analysis of the composites by X-ray photoelectron spectroscopy and high-resolution electron microscopy is presented.

I. Introduction

LASER synthesis of ceramic materials from gaseous precursors has generated considerable interest in recent years.[1] Haggerty *et al.*[2-5] suggest that silicon, Si_3N_4, SiC, and TiB_2 powders prepared by heating gaseous precursors with infrared radiation from a CO_2 laser have superior morphological properties as compared to powders prepared by conventional methods. In other work, Rice[6] has carried out the laser decomposition of 1,1,1,3,3,3-hexamethyldisilazane and isolated Si/C/N materials from the decomposition products. Each of these applications takes advantage of a strong infrared absorption band coincident with a wavelength of the CO_2 laser. Thus, silicon, Si_3N_4, and SiC were prepared from SiH_4, which absorbs at 10.59 μm. Rice utilized the coincidence between the 10P(20) CO_2 laser line and the symmetric stretch of ≡Si–N–Si≡ at 10.59 μm to decompose hexamethyldisilazane, $[(CH_3)_3Si]_2NH$, for the preparation of SiC/Si_3N_4 composites. Other examples of CO_2-laser-assisted preparation of powders include $FeSi_2$, FeSiC,[7] and SiB,[8] and boron-based materials such as B_4C,[9] B, and TiB_2.[10]

We have recently shown that tetrakis-(dimethylamino)titanium, $Ti[N(CH_3)_2]_4$, decomposes upon irradiation by 1.064-μm light from a pulsed Nd:YAG laser.[11] Broad-band visible emission from the vapor phase above the $Ti[N(CH_3)_2]_4$ sample accompanies the laser irradiation. As the laser intensity is increased, the emission develops structure indicating the formation of Ti and Ti^+. Both the visible emission and the formation of atomic titanium indicate multiphoton dissociation of $Ti[N(CH_3)_2]_4$ and/or its decomposition products.

In our previous work[11,12] which described the spectroscopy and dynamics of the laser-induced visible emission, we noted the formation of an amorphous gray-black residue upon prolonged irradiation of $Ti[N(CH_3)_2]_4$ at 1.064 μm, which could be pyrolyzed to TiN or TiN/TiC materials depending on firing conditions. We have employed this photodecomposition method to prepare a variety of TiN-containing composite materials. The impetus for this comes from the improved properties of composite materials. For example, TiN/TiO_2 composites are hard, heat-resistant, conductive materials which can be prepared by heating TiO_2 in an atmosphere of NH_3 and/or H_2.[13] Al_2O_3/TiN- and/or TiC-containing ceramics are high-strength materials,[14] while composites containing TiN in Si_3N_4 have been shown to have improved mechanical properties.[15] These powders are traditionally prepared by mechanically mixing the components, followed by high-temperature sintering; thus, there is a need for improved methods to prepare such materials which result in a better distribution of components.

The present paper describes experiments in which the photodecomposition of $Ti[N(CH_3)_2]_4$ is carried out in the presence of TiO_2, Al_2O_3, or Si_3N_4 powders. The residue adheres to the particles and forms TiN/metal oxide or TiN/Si_3N_4 composites on firing in a flowing NH_3/N_2 atmosphere. This synthetic route concentrates the titanium nitride on the surface of particles. The experimental conditions employed for the laser-assisted preparation of TiN composites are described. The composites have been studied by Raman spectroscopy and X-ray powder diffraction. X-ray photoelectron spectroscopy (XPS) and high-resolution electron microscopy (HREM), which are more surface sensitive, are used to determine the surface chemistry and structure of the composites.

II. Experimental Procedure

All materials used in these experiments were handled in either a dry box (argon atmosphere) or a high-vacuum system with nitrogen atmosphere using Schlenk techniques to exclude air and moisture.[16] Hexanes were carefully dried and stored over sodium-benzophenone ketyl. $Ti[N(CH_3)_2]_4$, a clear yellow liquid (bp 50°C/0.05 mtorr), was prepared according to a literature procedure.[17] Aluminum oxide and titanium oxide were obtained by hydrolysis of commerical aluminum tris(sec-butoxide) and tetrakis(2-propoxo)titanium, respectively, followed by pyrolysis at 800°C. XRD of the samples indicated that alumina is polycrystalline and titanium oxide is a mixture of two tetragonal phases crystallizing in the space groups *I*41/*amd* (141) and *P*42/*mnm* (136) (JCPD Card Nos. 21-1272 and 21-1276, respectively). Commercial Si_3N_4 (hexagonal, SG *P*31*c*(159), commonly called α-Si_3N_4), was used as received.

(1) Spectroscopic Measurements

The apparatus for the experiments is shown in Fig. 1. Laser 1 was used to dissociate $Ti[N(CH_3)_2]_4$ and, in the presence of the metal oxide or Si_3N_4 particles, to produce residue-coated particles. Laser 2 was used to demonstrate that the fluorescence observed along the laser beam path within the sample tube

R. W. Rice—contributing editor

Manuscript No. 194903. Received February 1, 1993; approved July 20, 1993.
Presented at the 4th Chemical Congress of North America and 202nd American Chemical Society National Meeting, New York, August 25–30, 1991 (Polymer Science Division, Paper No. 230).

*Chemistry Department, Ford Motor Company.
†Electron Microbeam Analysis Laboratory, The University of Michigan.
‡Physics Department, Ford Motor Company.
§Author to whom correspondence is to be addressed.

originates from multiphoton absorption of the 1.064-μm radiation. This laser excites, along the crossarm of the sample tube, the gaseous species formed by laser vaporization and/or ablation of $Ti[N(CH_3)_2]_4$ by laser 1 (distance from crossarm to sample is ~70 cm). Laser-induced fluorescence stimulated by laser 2 was collected and focused onto the entrance slits of a monochromator (HR320 0.32-m monochromator, Instruments SA, Metuchen, NJ). The dispersed emission spectrum was recorded by a gated, intensified, diode array detector (IPDA-700SB detector and ST1000 controller, Princeton Instruments, Trenton, NJ) at a specified time delay (0–5 μs) following the laser firing. A brief review of the emission spectra is given in Sect. III(1); a more complete discussion appears in Ref. 11.

(2) General Method for the Preparation of Composites

The composites were prepared by laser irradiation (laser 1) of a suspension of TiO_2, Al_2O_3, or Si_3N_4 in excess $Ti[N(CH_3)_2]_4$ using an apparatus similar to that in Fig. 1, except that a quartz tube (90 cm by 3.8 cm diameter) without side arms was used. The reaction tube was charged with either TiO_2, Al_2O_3, or Si_3N_4 and evacuated overnight. $Ti[N(CH_3)_2]_4$ was introduced into the sample tube with a syringe. The powders were kept in suspension by stirring. The reaction mixture was irradiated by the unfocused (beam diameter = 7 mm) 1.064-μm output of a Nd:YAG laser operating at 10 Hz with an energy output of approximately 600 mJ/pulse and a pulse width of 9 ns.

Over the course of several minutes, the titanium amide sample turned from clear yellow to opaque black. The irradiation was stopped and excess $Ti[N(CH_3)_2]_4$ and volatile decomposition products were distilled out of the reaction vessel under vacuum. The remaining dark gray-black free-flowing powders were fired in a flow of ammonia at 800°C. Samples from a second run were first pyrolyzed at 800°C in flowing ammonia. The temperature was then raised to 1100°C and the atmosphere was changed to flowing N_2. The samples, thus prepared, are labeled $TiN/M_nX_m/800$ or $TiN/M_nX_m/1100$, (M_nX_m = Al_2O_3, TiO_2, or Si_3N_4) based on thermal treatment. The loading of TiN was calculated based on the consumed $Ti[N(CH_3)_2]_4$.

Experiments were carried out to find a tentative correlation between irradiation time and TiN loading. In the first set of experiments, the irradiation was stopped after 10 min, and the TiN loading was found to be ~7.5%. Irradiation of the samples for 45 min increased the loading to ~14%. Significant increases in loading by prolonged irradiation were hampered, with the current apparatus, by a buildup of a film of decomposition products on the window, which reduced the radiation intensity reaching the samples.

(A) TiN/TiO_2 Powders: After laser irradiation of a suspension of TiO_2 (0.5 g) in $Ti[N(CH_3)_2]_4$ (1.92 g), excess $Ti[N(CH_3)_2]_4$ (1.28 g) was recovered by distillation and the residue was pyrolyzed. The samples are referred to as $TiN/TiO_2/800$ and $TiN/TiO_2/1100$. TiN loading is 24% (w/w).

(B) TiN/Al_2O_3 Powders: The irradiation of Al_2O_3 (0.5 g) in $Ti[N(CH_3)_2]_4$ (1.92 g) yielded residue-coated particles and 1.35 g of recovered $Ti[N(CH_3)_2]_4$, implying a TiN loading of 25.8% (w/w). The residue was pyrolyzed to form composites. The coated particles are labeled $TiN/Al_2O_3/800$ and $TiN/Al_2O_3/1100$.

(C) TiN/Si_3N_4 Powders: 0.5 g of Si_3N_4 was irradiated in 1.92 g of $Ti[N(CH_3)_3]_4$, leaving 1.31 g of excess $Ti[N(CH_3)_2]_4$; thus, the TiN loading is 25% (w/w). The composite formed on pyrolysis is labeled $TiN/Si_3N_4/1100$.

III. Results and Discussion

(1) Decomposition Dynamics

The near-IR spectrum of $Ti[N(CH_3)_2]_4$ reveals a series of very weak absorption peaks in the vicinity of 1 μm. The laser wavelength of 1.064 μm, however, lies to the short-wavelength side of these features at which the measured extinction cross section is less than 7×10^{-23} cm^2, most of which is probably due to reflective losses rather than absorption. This is consistent with our observation that the 1.064-μm laser radiation initially passes through the titanium amide sample (in the absence of metal oxide particles) with little loss. Over the course of a few minutes, at a laser intensity of 1.6×10^8 W·cm^{-2}, the initially clear yellow $Ti[N(CH_3)_2]_4$ begins to turn brown. Concurrently, an intense laser-induced fluorescence develops along the entire length of the sample tube. Figure 2 shows emission spectra at two laser intensities. At the lower intensity, broadband emission is observed over the range of 350–700 nm; higher intensity irradiation produces structure in the emission spectrum corresponding to known Ti and Ti^+ emission lines.[18]

The laser-induced fluorescence spectra shown in Fig. 2 result from multiphoton absorption by $Ti[N(CH_3)_2]_4$ and/or its titanium- and nitrogen-containing molecular fragments which have been decomposed and volatilized by laser 1. This assertion can be substantiated by a number of observations. The excited states which lead to emission in the 355–532-nm range can be reached only by the absorption of at least three 1.064-nm photons; a minimum of two photons are required for emission in the 532–700 nm range. The dependence of fluorescence intensity on laser power is consistent with such multiphoton absorption.[11] The emission is not due to laser ablation or pyrolysis of the titanium amide, since, after a few minutes irradiation of the sample by laser 1, the emission spectra in Fig. 2 are observed along the crossarm of the sample tube upon the firing of laser 2. The emission arising from the firing of laser 2 can be observed even an hour after irradiation by laser 1 has ceased, indicating that the

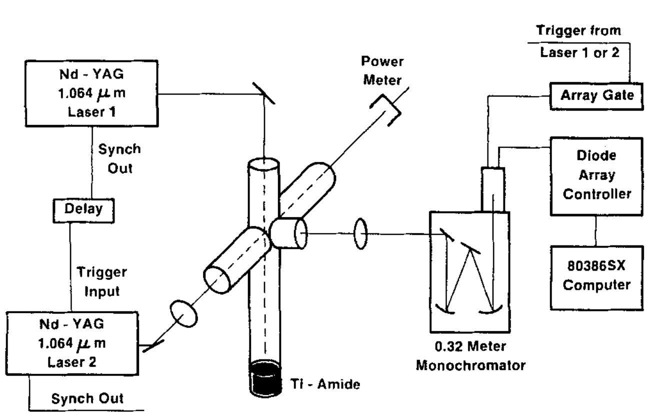

Fig. 1. Apparatus for laser-assisted decomposition of $Ti[N(CH_3)_2]_4$ and spectroscopic measurements.

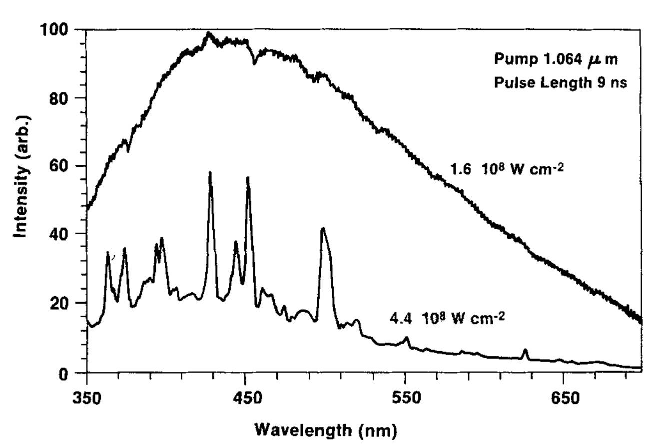

Fig. 2. Laser-induced fluorescence spectra of $Ti[N(CH_3)_2]_4$ and/or its decomposition fragments. The excitation wavelength is 1.064 μm.

emission arises from chemically stable species. The emission arises from $Ti[N(CH_3)_2]_4$ and/or its titanium- and nitrogen-containing molecular fragments, because emission spectra very similar to those shown in Fig. 2 are obtained from the irradiation of $(CH_3)_3Si(H)NTiCl_3$[19] and even TiN, whereas no fluorescence is observed upon the irradiation of $TiCl_4$, $Ti(i\text{-}C_3H_7O)_4$, $B[N(CH_3)_2]_3$, or $Si[N(CH_3)_2]_4$.[11] Finally, the observation of atomic emission lines from titanium and the formation of a black coating along the sides of the sample cell imply that not only multiphoton absorption, but also multiphoton dissociation occurs.

The above observations pertain to the vapor phase above the titanium amide sample. That the same laser absorption/decomposition processes occur in the liquid phase is supported by experiments carried out in dilute solutions (0.001*M*) of $Ti[N(CH_3)_2]_4$ in hexane. These experiments reveal laser-induced fluorescence spectra very similar to those shown in Fig. 2; decomposition is evidenced by the pale yellow solution turning brown. We should note, however, that with the $Ti[N(CH_3)_2]_4$/metal oxide or silicon nitride mixtures used to coat the particles in the first step of our laser-assisted composite preparation, laser pyrolysis could also play a role. This is because the suspensions in titanium amide become (after approximately 5–10 min) essentially opaque to 1.064-μm radiation, in which case significant local heating of the sample could take place.

The major dissociation products obtained after 1.064-μm irradiation of $Ti[N(CH_3)_2]_4$ are dimethylamine, tetramethylhydrazine (as revealed by GC-mass spectroscopy and NMR spectroscopy) and an insoluble, gray-black, residue.[¶] A pyrolytic pathway could explain the formation of dimethylamine.[21]

$$Ti[N(CH_3)_2]_4 \xrightarrow{\Delta} \overline{Ti[N(CH_3)_2]_2[NCH_2}CH_3] + (CH_3)_2NH$$

However, the appearance of N,N,N′,N′-tetramethylhydrazine suggests that $(CH_3)_2N^\cdot$ free radicals are formed and further corroborates the multiphoton dissociation hypothesis.

$$Ti[N(CH_3)_2]_4 \xrightarrow{h\nu} [(CH_3)_2N]_3Ti^\cdot + (CH_3)_2N^\cdot$$

$$2(CH_3)_2N^\cdot \longrightarrow (CH_3)_2N^\cdot N(CH_3)_2$$

In a separate experiment, we found that the dimethylamine does not itself undergo decomposition on exposure to 1.064-μm laser radiation, thus ruling out the possibility that the dimethylamine free radicals originate from pyrolysis of $Ti[N(CH_3)_2]_4$, followed by a dissociation of $(CH_3)_2NH$. Instead, the dimethylamine could arise as a result of hydrogen abstraction from the dimethylamino groups by dimethylamine radicals.

The formation of dimethylamine and N,N,N′,N′-tetramethylhydrazine suggests that the residue which coats the sample tube likely arises from the recombination of free radicals generated by the laser-induced multiphoton dissociation. The observation of absorption bands in the 2800–3000-cm^{-1} C–H stretching region in the IR spectrum (Galaxy Series FTIR 5000 spectrometer, Mattson Instruments, Inc., Madison, WI) of the residue indicates that it contains organic groups. A reproducible elemental analysis of the residue could not be obtained (e.g., C 23.6%, H 4.4%, Ti 29.2%, N 9.3%, total accounted mass 66.5%, analyzed by Galbraith Laboratories, Knoxville, TN). The residue could be either an oligomer, a polymer, or a mixture of species. A thermogravimetric analysis of the residue shows a weight loss of 35% in the temperature range 50°–400°C, a 9% weight decrease in the 600°–720°C range, and no further weight loss in the 720°–900°C range. This suggests that the residue contains substantial organic groups.

When the residue is fired at 800°C in a nitrogen or ammonia atmosphere, it yields a powder which is identified by X-ray powder diffraction (XRD) (PAD V XRD, Scintag, Santa Clara, CA) to be a mixture of TiN and TiC in 5:1 ratio. This powder can be converted to pure TiN by firing in an ammonia atmosphere at 1100°C for 2 h. The yield of TiN is 77%, based on decomposed $Ti[N(CH_3)_2]_4$ (undecomposed $Ti[N(CH_3)_2]_4$ was distilled out of the reaction vessel to obtain an accurate value for decomposed $Ti[N(CH_3)_2]_4$). The XRD pattern of the dark olive-brown powder showed diffraction peaks at 2θ (intensity) = 42.8(100), 62.0(65), 36.8(54), 74.2(10), 78.2(7), which are in complete agreement with those reported for titanium nitride (JCPD Card No. 38-1420).

[¶]Lesser amounts of bis-(dimethylamino)methane and some low molecular weight hydrocarbons are also found in the volatile fraction.

(2) *Characterization of the* TiN/Al_2O_3, TiN/TiO_2, *and* TiN/Si_3N_4 *Composites*

The preparation of TiN/TiO_2, TiN/Al_2O_3, and TiN/Si_3N_4 composites involves irradiation of a suspension of TiO_2, Al_2O_3, or Si_3N_4 particles in excess $Ti[N(CH_3)_2]_4$ with 1.064-μm laser light, recovery of the excess $Ti[N(CH_3)_2]_4$ by distillation, followed by firing of the residue-coated particles. The particles act as substrates onto which solid decomposition products of the laser decomposition adhere. Firing the coated particles removes the remaining organic groups and furnishes composites with a uniform TiN distribution.

The coated TiO_2 and Al_2O_3 samples prepared at 800°C are suitable for HREM studies. Based on the X-ray powder diffraction results below, the coated Al_2O_3 particles were selected for HREM examinations. The coated Si_3N_4 particles were not subjected to this heat treatment, because the particles are thick and are not suitable for HREM studies.

X-ray powder diffraction of $TiN/TiO_2/800$ shows diffraction peaks for tetragonal TiO_2, which crystallizes in the space group *P42/mnm* (136) (JCPD Card No. 21-1276). TiN diffraction peaks are not seen, due to the poor crystallanity of the TiN. TiN/Al_2O_3/800 particles, on the other hand, exhibit broad TiN and γ-alumina (JCPD Card No. 29-63, cubic, SG *F*) diffraction peaks. The broad alumina peaks are due to its crystallization in γ-form and the small particle size. We also examined these samples by XPS and found the binding energy of C 1*s* to be 286 eV, suggesting the absence of titanium carbide (binding energy 281.8 eV[24]). It is possible that metal oxide substrates facilitate reduction of organic groups, thus preventing formation of titanium carbide.

The samples of coated TiO_2, Al_2O_3, and Si_3N_4 were fired at 1100°C to induce TiN crystallization and crystal growth. The loading of TiN was calculated to be in the 24%–26% range, based on consumed $Ti[N(CH_3)_2]_4$. The samples were analyzed by Raman spectroscopy and X-ray powder diffraction studies.

(A) Raman Spectroscopy: Powders of TiN are highly absorbing in the visible range and are thus susceptible to laser-induced oxidation when illuminated with a high-power laser typically used for Raman studies[22] (514.5-nm Ar laser, Spectra-Physics, Mountain View, CA; triple monochromator, SPEX Instruments, Metuchen, NJ; array detector system, EG&G PAR, Princeton, NJ). To prevent any laser-induced effects, we used 2 mW of laser power focused to a spot size of 50–100 μm^2. The resulting power density on the samples was roughly four orders of magnitude below that needed to induce oxidation.[22] Long exposure times, ~30 min, were used to obtain spectra with adequate signal-to-noise ratios.

There are no first-order-allowed Raman active modes associated with the rock salt structure of TiN, and its spectrum contains no sharp lines. The Raman signature of TiN corresponds to weak defect-induced bands that crudely match the one-phonon density-of-states.[23] Second-order scattering can also be observed, but these features are even weaker than the defect-induced bands. The spectra that best showed the characteristic fingerprint of TiN were obtained on the TiN–Al_2O_3 composites, an example of which is shown in Fig. 3. The broad band extending from 200 to 340 cm^{-1} corresponds to the acoustic phonons, whereas the narrower band centered near 540 cm^{-1} corresponds to optical phonons. These features are indicated by the vertical arrows in Fig. 3, and they match well the TiN

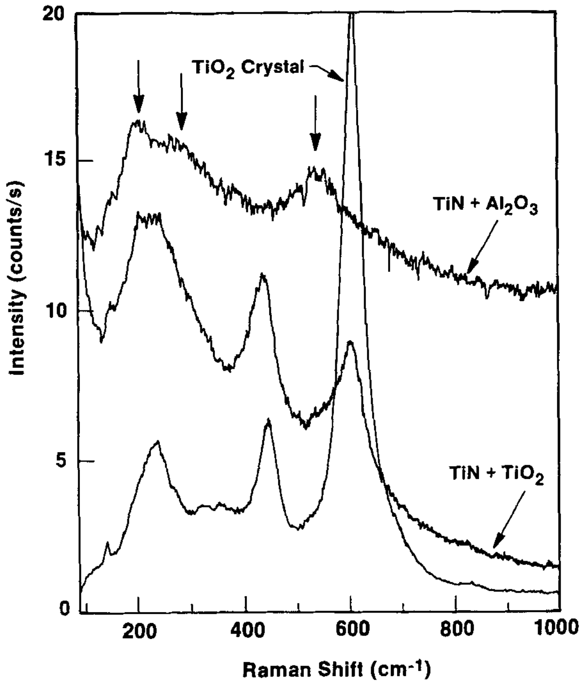

Fig. 3. Raman spectra of $TiN/Al_2O_3/1100$, $TiN/TiO_2/1100$, and TiO_2.

Raman features reported by Spengler and Kaiser.[23] There is no interference from the γ-Al_2O_3, which is amorphous and gives no observable Raman lines. The spectrum in Fig. 3 also confirms the absence of α-Al_2O_3, which would have several sharp lines in this spectral region. The frequency of the first peak in the acoustical range has been shown to depend on the Ti/N ratio.[23] The observed frequency at 200 cm^{-1} corresponds to stoichiometric TiN.

The Raman spectra of the TiN-TiO_2 composites (Fig. 3) also indicated the presence of TiN. In this case, however, there is strong interference from the TiO_2 lines. Spectra from the composite and a single crystal of the rutile phase of TiO_2 are shown in Fig. 3. The presence of TiN in the spectrum from the composite is indicated by the broadened and shifted band in the 200–300-cm^{-1} region and the shoulder on the low-frequency side of the 610-cm^{-1} TiO_2 line. The TiN–Si_3N_4 composites gave a fluorescence signal roughly 10^2 larger than the other samples, preventing us from obtaining any useful Raman spectra.

(B) X-ray Diffraction: The X-ray powder diffraction patterns of $TiN/TiO_2/1100$, $TiN/Al_2O_3/1100$, and $TiN/Si_3N_4/1100$ are shown in Fig. 4 and the assignment of diffraction peaks is presented in Tables I–III. $TiN/TiO_2/1100$ shows TiN diffraction peaks for cubic TiN, crystallized in space group *Fm3m* (225) (JCPD Card No. 38-1420) along with peaks corresponding to TiO_2. The γ-alumina and TiN diffraction peaks are broad in the XRD of $TiN/Al_2O_3/1100$, suggesting that titanium nitride is stabilizing alumina in the γ-phase. $TiN/Si_3N_4/1100$ shows strong diffraction peaks for α-Si_3N_4 (JCPD Card No. 41-360, hexagonal, SG *P*31*c* (159)) and weak broad peaks for TiN. The particle sizes for the TiN component in $TiN/TiO_2/1100$, $TiN/Al_2O_3/1100$, and $TiN/Si_3N_4/1100$ samples have been calculated by Scherrer's formula to be 1050, 223, and 300 Å, respectively.

Thus, the Raman spectra and X-ray powder diffraction patterns of the composites show the presence of titanium nitride in TiN/Al_2O_3, TiN/TiO_2, and TiN/Si_3N_4 composites. Further studies by X-ray photoelectron spectroscopy (XPS) and high-resolution transmission electron microscopy show that titanium nitride is concentrated on the surface of metal oxide or silicon nitride particles.

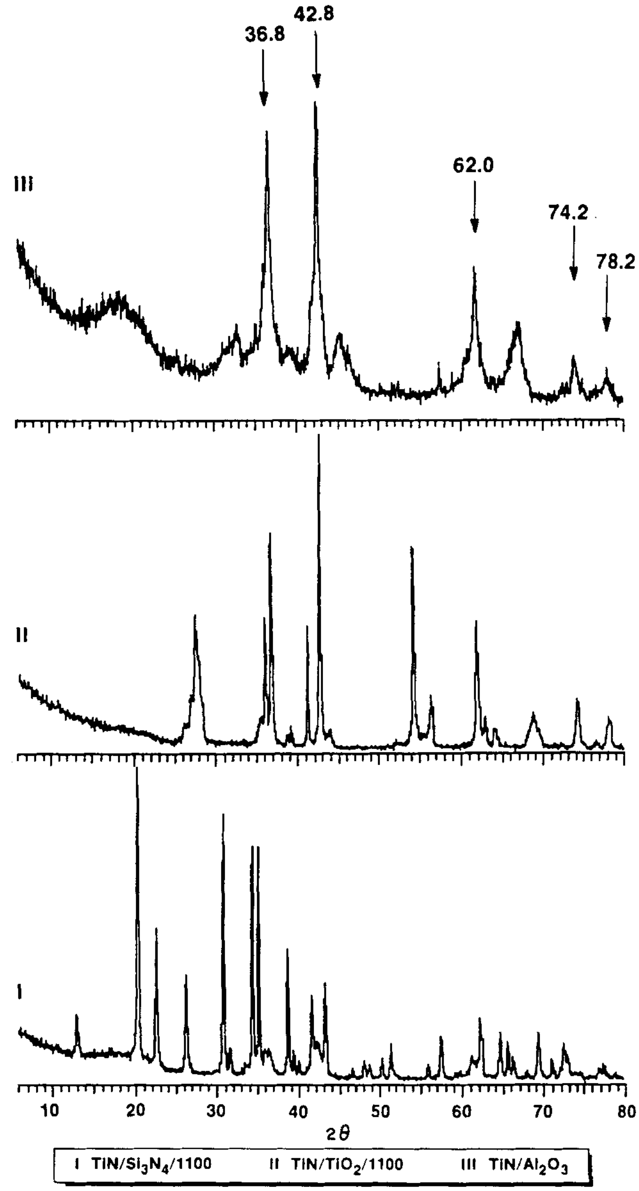

Fig. 4. X-ray powder diffraction of composites. The arrows indicate the positions of TiN diffraction peaks.

Table I. X-ray Powder Diffraction Data for TiN/TiO_2 Powders*

$TiN/TiO_2/800$ (2θ(I))	$TiN/TiO_2/1100$ (2θ(I))	Assignments (*hkl*)
27.5(88)	27.3(42)	TiO_2(110)
36.0(55)	35.9(41)	TiO_2(101)
	36.6(67)	TiN(111)
38.2(44)	39.02(8)	TiO_2(200)
41.0(25)	41.1(37)	TiO_2(111)
	42.6(100)	TiN(200)
44.4(9)	44.0(6)	TiO_2(210)
54.4(100)	54.2(64)	TiO_2(211)
56.8(22)	56.4(16)	TiO_2(220)
	61.9(39)	TiN(220)
62.7(20)	62.9(10)	TiO_2(002)
64.2(11)	64.1(7)	TiO_2(310)
68.9(40)	68.7(12)	TiO_2(301)
69.8(12)	69.5(8)	TiO_2(112)
	74.1(16)	TiN(311)
	78.1(10)	TiN(222)

*Assignments are based on values from JCPD files for TiN (Card No. 38-1420) and TiO_2 (Card No. 21-1276).

Table II. X-ray Powder Diffraction Data for TiN/Al_2O_3 Powders*

TiN/Al_2O_3/800 (2θ)†	TiN/Al_2O_3/1100 (2θ)‡	Assignments (*hkl*)
	18.4(40)	Al_2O_3(111)
	32.5(30)	Al_2O_3(220)
36.5(82)	36.5(89)	TiN(111)
	39.2(23)	Al_2O_3(222)
42.8(100)	42.4(100)	TiN(200)
46.0(35)	45.3(28)	Al_2O_3(400)
	60.4(20)	Al_2O_3(511)
62.0(50)	61.7(47)	TiN(220)
67.1(52)	67.1(30)	Al_2O_3(440)
	74.0(20)	TiN(311)
	77.9(15)	TiN(222)

*Assignments are based on values from JCPD files for TiN (Card No. 38-1420) and Al_2O_3 (Card No. 29-63). †TiN/Al_2O_3/800 is poorly crystalline and does not exhibit alumina peaks. There is a peak at 35.7°, which could not be assigned. ‡The alumina peaks are broad in the diffraction pattern of TiN/Al_2O_3/1100. There are also very weak, sharp diffraction peaks at 2θ = 25.4, 34.9, 52.4, 57.4, 58.8, and 72.6, indicating initiation of conversion of γ-alumina to α-alumina (JCPDS Card No. 10-173).

Table III. X-ray Powder Diffraction Data for TiN/Si_3N_4 Powders*

TiN/Si_3N_4/1100 (2θ(I))	Assignments (*hkl*)
13.0(21)	Si_3N_4(100)
20.4(100)	Si_3N_4(101)
22.8(48)	Si_3N_4(110)
26.4(34)	Si_3N_4(200)
30.8(84)	Si_3N_4(201)
31.7(12)	Si_3N_4(002)
34.5(75)	Si_3N_4(102)
35.2(75)	Si_3N_4(210)
36.5(11)	TiN(111)
38.8(42)	Si_3N_4(211)
39.5(10)	Si_3n_4(112)
40.1(7)	Si_3N_4(300)
41.8(28)	Si_3N_4(202)
42.3(14)	TiN(200)
43.4(32)	Si_3N_4(301)
46.7(5)	Si_3N_4(220)
48.2(7)	Si_3N_4(212)
48.8(7)	Si_3N_4(310)
50.4(8)	Si_3N_4(103)
51.6(12)	Si_3N_4(311)
57.6(15)	Si_3N_4(222)
60.0(4)	Si_3N_4(320)
61.4(8)	TiN(220) + Si_3N_4(213)
62.4(20)	Si_3N_4(321)
64.7(16)	Si_3N_4(303)
65.7(13)	Si_3N_4(411)
66.4(9)	Si_3N_4(004)
69.5(16)	Si_3N_4(322)

*Assignments are based on values from JCPD files for TiN (Card No. 38-1420) and Si_3N_4 (Card No. 41-360).

(C) X-ray Photoelectron Spectroscopic Studies: XPS of TiN/TiO_2/1100, TiN/Al_2O_3/1100, and TiN/Si_3N_4/1100 show the presence of Ti, N, C, O and the metal from the substrate (Ti, Al, or Si). The binding energy of *C* 1*s* in all three samples is at 286 eV, suggesting the absence of titanium carbide (281.8 eV[24]). The titanium and nitrogen regions of the XPS of TiN/TiO_2/1100 are shown in Fig. 5. TiN/TiO_2/1100 exhibits Ti $2p_{3/2}$ peaks at 455.5 and 459 eV for TiN and TiO_2, respectively. There is an unresolved region between TiN and TiO_2 centered at 457 eV due to titanium oxynitride.[25-27] The Ti $2p_{3/2}$ regions for the samples TiN/Al_2O_3/1100 and TiN/Si_3N_4/1100 are unresolved and consist of peaks due to TiN, TiO_2, and titanium oxynitride. These features have previously been observed in XPS studies of unetched titanium nitride coatings.[27]

The N 1*s* peaks in all three samples are observed at 397 eV and are assigned to titanium nitride. In the case of TiN/Si_3N_4/1100, the N 1*s* peaks for TiN and Si_3N_4 are not resolved. All three samples show small unresolved components at 399 eV, which could be due to nitrogen contaminants or titanium oxynitride.[27]

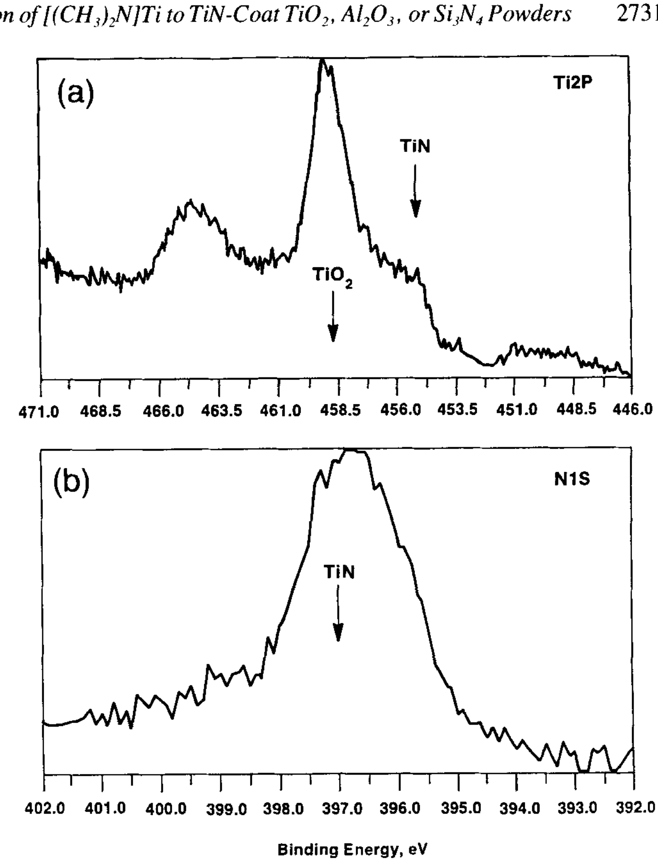

Fig. 5. XPS of TiN/TiO_2/1100: (a) titanium window—the positions of Ti peaks for TiN and TiO_2 are indicated by arrows; (b) nitrogen window—the position of N peak for TiN is indicated by an arrow.

It should be pointed out that Porte *et al.*[28] have shown that the binding energy difference between the Ti 2*p* and N 1*s* peaks is linearly related to the concentration of nitrogen in the range TiN/N = 0.5–1.0. Thus Ti 2*p* peak broadening could also result due to the presence of several nonstoichiometric TiN species on the surface.

These results, thus, support the formation of titanium nitride and the absence of titanium carbide on the composite particles. The expected surface contamination of the composites due to oxidation/nonstoichiometric TiN is also seen in the spectra. Such surface oxidation has previously been observed by several authors in TiN films prepared by CVD.[25-27]

(D) Transmission Electron Microscopy Studies: The TiN/TiO_2/800 and TiN/Al_2O_3/800 samples were examined by conventional transmission electron microscopy (TEM) (CR12 AEM, Philips, Mahwah, NJ) and the latter by high-resolution electron microscopy (HREM) (4000EX HREM, JEOL, Peabody, MA). Both samples have a particle thickness of less than 20 nm and can be studied directly by HREM without the need to thin the sample.[29]

TEM examination of TiN/TiO_2/800 showed small particles with well-defined boundaries. Energy-dispersive spectra (EDS) of several individual particles exhibited Ti, N, and O peaks. TiN/Al_2O_3/800 particles were found to occur as small particle agglomerates. Several of these were examined via EDS, which revealed titanium $K\alpha$, $K\beta$ and L_0 peaks, as well as the nitrogen $K\alpha$ peak. Figure 6 shows a HREM micrograph of the TiN/Al_2O_3/800 sample. Several individual particles on the order of 5 nm in diameter can be distinguished (indicated by arrows). Figure 6(b) is an enlargement of one such particle. Figure 6(c) is the corresponding Fourier transform power spectrum.[30]

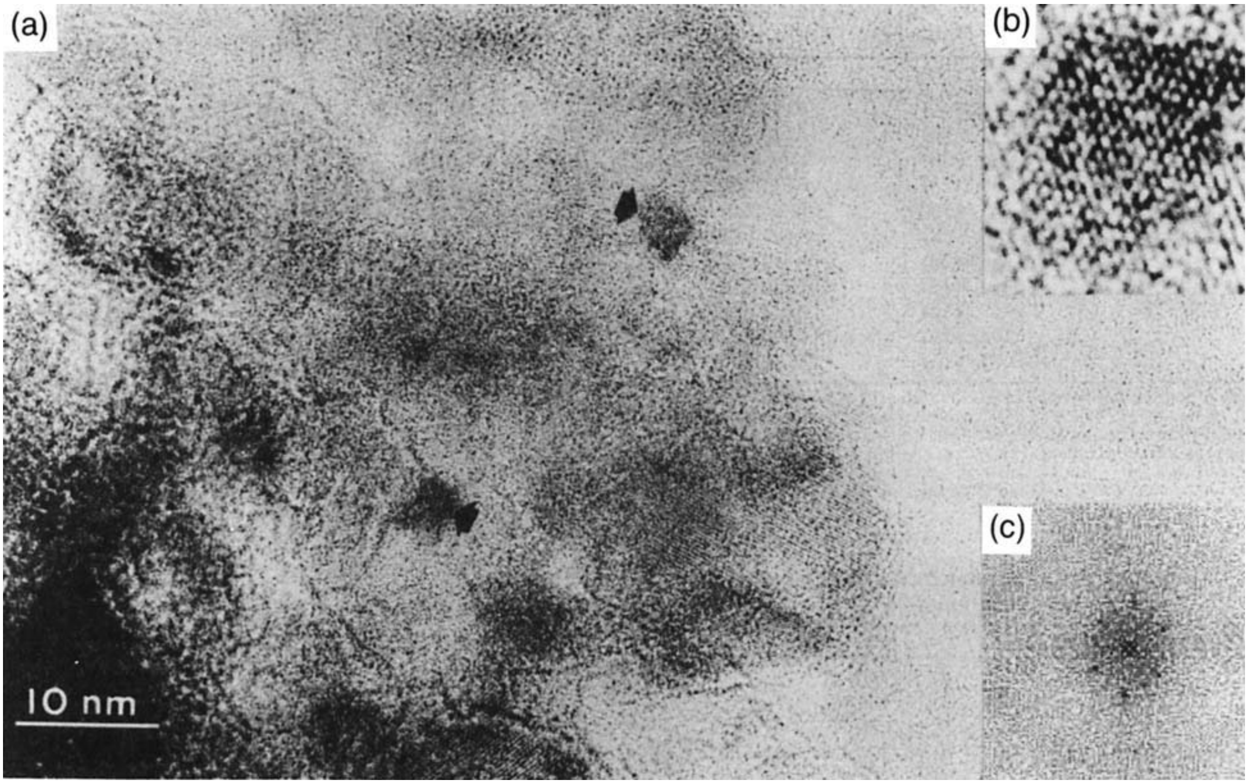

Fig. 6. (a) HREM image of $TiN/Al_2O_3/800$ particles; note the presence of several small particles indicated by arrows. (b) Enlargement at one such point. (c) Corresponding power spectrum indicating a ⟨011⟩ fcc zone axis.

The aspect ratio of this pattern closely matches that of a face-centered-cubic structure, looking along a ⟨011⟩ type zone axis. Measurements of the reciprocal lattice vectors of this pattern were calibrated with reference to similar measurements of the [011] zone axis power spectrum from a silicon standard. Results indicate interplanar spacing of 0.245 and 0.213 nm, which compare favorably with {111} and {002} spacings of TiN (JCPDS Card No. 38-1420). Since atomic structure images arise from areas within 5–10 nm of the free surface, these particles must reside in the region near the surface.

IV. Conclusions

Irradiation of tetrakis-(dimethylamino)titanium by the 1.064-μm fundamental of a Nd:Yag laser results in its decomposition, yielding amongst other products a gray-black solid residue. The residue can be converted to TiN or TiN/TiC, depending on firing conditions. When TiO_2, Al_2O_3, or Si_3N_4 particles are present, the residue adheres to the particles, and TiN/TiO_2, TiN/Al_2O_3, and TiN/Si_3N_4 composites are formed upon firing the residue-covered particles. The XPS and HREM studies show that the TiN component is near the surface of the particles.

Acknowledgments: The use of the Philips CM12/STEM and JEOL 4000EX electron microscopes and Perkin-Elmer XPS 5400 at the Electron Microbeam Laboratory, University of Michigan, Ann Arbor, MI, is gratefully acknowledged. CKN also thanks Mr. H. Estry for assistance in XPS data collection and helpful suggestions.

References

[1]J. S. Haggerty and W. R. Cannon, "Sinterable Powders from Laser-Driven Reactions"; pp. 165–241 in *Laser-Induced Chemical Processes*. Edited by J. I. Steinfeld. Plenum Press, New York, 1981.

[2]W. R. Cannon, S. C. Danforth, J. H. Flint, J. S. Haggerty, and R. A. Marra, "Sinterable Ceramic Powders from Laser-Driven Reactions: I, Process Description and Modeling," *J. Am. Ceram. Soc.*, **65** [7] 324–30 (1982).

[3]W. R. Cannon, S. C. Danforth, J. S. Haggerty, and R. A. Marra, "Sinterable Ceramic Powders from Laser-Driven Reactions: II, Powder Characteristics and Process Variables," *J. Am. Ceram. Soc.*, **65** [7] 330–35 (1982).

[4]H. Flint and J. S. Haggerty, "Ceramic Powders from Laser Driven Reactions," *Proc. Soc. Photo-Opt. Instrum. Eng.*, **458**, 108–13 (1984).

[5]Y. Suyama, R. A. Marra, J. S. Haggerty, and H. K. Bowen, "Synthesis of Ultrafine SiC Powders by Laser-Driven Gas Phase Reactions," *Am. Ceram. Soc. Bull.*, **64** [10] 1356–59 (1985).

[6]G. W. Rice, "Laser Synthesis of Si/C/N Powders from 1,1,1,3,3,3-Hexamethyldisilazane," *J. Am. Ceram. Soc.*, **69** [8] C-183–C-185 (1986).

[7]A. Gupta and J. T. Yardley, "Production of Light Olefins from Synthesis Gas Using Catalyst Prepared by Laser Pyrolysis," in *Applications of Lasers to Industrial Chemistry, Proc. SPIE—Int. Soc. Opt. Eng.*, **458**, 131–39 (1984).

[8]A. Gupta, G. A. West, and J. P. Donlan, "Boron Diffusion in Silicon from Ultrafine Boron–Silicon Powders," in *Laser Assisted Deposition, Etching, and Doping, Proc. SPIE—Int. Soc. Opt. Eng.*, **459**, 94–102 (1984).

[9]A. K. Knudsen, "Laser Driven Synthesis and Densification of Ultrafine Boron Carbide Powders"; pp. 237–47 in Advances in Ceramics, Vol. 21, *Ceramic Powder Science*. Edited by G. L. Messing, K. S. Mazdiyasni, J. W. McCauley, and R. A. Haber. American Ceramic Society, Westerville, OH, 1987.

[10]J. D. Casey and J. S. Haggerty, "Laser Induced Vapor Phase Synthesis of Boron and Titanium Diboride Powders," *J. Mater. Sci.*, **22** [2] 737–44 (1987).

[11]M. M. Maricq and C. K. Narula, "1.064 μm Multiphoton Laser Induced Fluorescence and Dissociation of Tetrakis-(dimethylamino)titanium(IV)," *Chem. Phys. Lett.*, **187**, 220–26 (1991).

[12]C. K. Narula and M. M. Maricq, "Laser Induced Decomposition of Precursors Containing M–N Bonds for the Preparation of Metal-Nitride Preceramics, Powders and Coatings," *Am. Chem. Soc., Div. Polym. Chem.*, **32**, 499–500 (1991).

[13](a) T. Miyazaki, "Titanium Nitride–Titanium Oxide Composite Powder," *Jpn. Kokai Tokkyo Koho* JP 60 264 313 [85 264 313] CA **104** (1986) 151826. (b) M. Yoshizumi and S. Miyama, "Sintered Bodies Consisting of Surface Titanium Nitride and Internal Titanium Oxynitride," *Jpn. Kokai Tokkyo Koho* JP 60 200 862 [85 200 862] CA **104** (1986) 134831. (c) I. Norihiro, K. Maruyama, F. Nakamura, N. Kawamura, and N. Kuramitsu, "Manufacture of Metal Nitrides," *Jpn. Kokai Tokkyo Koho* JP 61 111 903 [86 111 903] CA **105** (1986) 99943.

[14](a) Mitsubishi Metal Corp., "High-Strength Alumina-Based Ceramics," *Jpn. Kokai Tokkyo Koho* JP 81 114 864 CA **96** (1982) 56809; (b) M. T. Laugier, "Surface Toughening of Ceramics," *J. Mater. Sci. Lett.*, **5**, 252 (1986), (c) J. Wernisch, W. Werner, C. Nissel, and B. Lux, "Diffusion at Aluminum Oxide/Titanium Carbide Phase Boundaries," *Sprechsaal*, **118**, 921 (1985).

[15]R. L. Allor, G. M. Crosbie, E. L. Cartwright, and R. K. Govila, "Silicon Nitride Based Ceramic Composites"; pp. 555–62 in Proceedings of Sixth Annual ASM/ESD Advanced Composites Conference (Detroit, MI, 1990). ASM International, Metals Park, OH, 1990.

[16]D. F. Shriver, *The Manipulation of Air-Sensitive Compounds*. McGraw-Hill, New York, 1967.

[17]D. C. Bradley and I. M. Thomas, "Metallo-Organic Compounds Containing Metal–Nitrogen Bonds. Part I. Some Dialkylamino-Derivatives of Titanium and Zirconium," *J. Chem. Soc.*, **3857** (1960).

[18]W. F. Meggers, C. H. Corliss, and B. F. Scribner, *Tables of Spectral Line Intensities*, NBS Monograph 145, part 1. National Bureau of Standards, Gaitersburg, MD, 1975.

[19]C. K. Narula, "New Routes to Group IVa Metal-Nitrides," *Mater. Res. Soc. Symp. Proc.*, **271,** 881–86 (1992).

[20](Deleted)

[21](a) M. F. Lappert and A. R. Sanger, "Amido-Derivatives of Metals and Metalloids. Part XIII. Dialkylamides of Low-Valent Titanium: their Preparation and Properties," *J. Chem. Soc. (A)*, 877–74 (1971). (b) W. A. Kornicker, E. P. Benzing, and E. Parry, "Titanium Amide Borohydrides and Chlorides and Their Use as Polymerization Catalyst," U.S. Pat. No. 3 394 156, 1968; (b) C. A. **69,** P67900, 1969; (c) G. S. Girolami, J. A. Jensen, J. E. Gozum, and D. M. Pollina, "Tailored Organometallics as Low-Temperature CVD Precursors to Thin Films," *Mater. Res. Soc. Symp. Proc.*, **121** 429–38 (1988).

[22]G. M. Begun and C. E. Bamberger, "Raman Spectroscopic Observation of Laser-Induced Oxidation of Transition-Metal Borides, Carbides, and Nitrides," *Appl. Spectrosc.*, **43,** 134–38 (1989).

[23](a) W. Spengler and R. Kaiser, "First and Second Order Raman Scattering in Transition Metal Compounds," *Solid State Commun.*, **18,** 881–84 (1976); (b) W. Spangler, R. Kaiser, A. N. Christensen, and G. Müller-Vogt, "Raman Scattering, Superconductivity, and Phonon Density of States of Stoichiometric and Non-Stoichiometric TiN," *Phys. Rev. B: Condens. Matter*, **17,** 1095–101 (1978).

[24](a) H. Ihara, Y. Kumashiro, A. Itoh, and K. Maeda, "Some Aspects of ESCA Spectra of Single Crystals and Thin Films of Titanium Carbide," *Jpn. J. Appl. Phys.*, **12** [9] 1462–63 (1973). (b) G. S. Girolami, J. A. Jensen, and D. B. Pollina, "Organometallic Route to the Chemical Vapor Deposition of Titanium Carbide Films at Exceptionally Low Temperatures," *J. Am. Chem. Soc.*, **109,** 1579–80 (1987).

[25]K. S. Robinson and P. M. A. Sherwood, "X-ray Photoelectron Spectroscopic Studies of the Surface of Sputter Ion Plated Films," *SIA, Surf. Interface Anal.*, **6** [6] 261–66 (1984).

[26]N. Heide, B. Siemensmeyer, and J. W. Schultze, "Surface Characterization and Electrochemical Behavior of Nitrogen and Carbon-implanted Titanium," *SIA, Surf. Interface Anal.*, **19,** 423–29 (1992).

[27](a) R. Bertoncello, A. Casagrande, M. Casarin, A. Glisenti, E. Lanzoni, L. Mirenghi, and E. Tondello, "TiN, TiC and Ti(C,N) Film Characterization and Its Relationship to Tribological Behavior," *SIA, Surf. Interface Anal.*, **18** [7] 525–31 (1992); (b) R. Fix, R. G. Gordon, and D. M. Hoffman, "Chemical Vapor Deposition of Titanium, Zirconium, and Hafnium Nitride Thin Films," *Chem. Mater.*, **3,** 1138–48 (1991).

[28]L. Porte, L. Roux, and J. Hanus, "Vacancy Effects in the X-ray Photoelectron Spectra of TiN_x," *Phys. Rev. B: Condens. Matter*, **28,** 3214–24 (1983).

[29]A. K. Datye, R. T. Paine, C. K. Narula, and L. F. Allard, "Novel Approach for High-Resolution TEM Studies of Ceramic–Ceramic Interfaces," *Mater. Res. Soc. Symp. Proc.*, **153,** 97–102 (1989).

[30]J. Cowley, *Diffraction Physics*; 2nd rev. ed; pp. 35–49. North Holland Physics Publishing Company, New York, 1984. □